(2)

MTL TR 90-63

AD

AD-A231 969

A DETERMINATION/VALIDATION OF AUTOCLAVE FORCED CONVECTION HEATING

STEVEN M. SERABIAN
MECHANICS AND STRUCTURES BRANCH

DONALD J. JAKLITSCH
COMPOSITES DEVELOPMENT BRANCH

December 1990

US ARMY
LABORATORY COMMAND
MATERIALS TECHNOLOGY LABORATORY

U.S. ARMY MATERIALS TECHNOLOGY LABORATORY
Watertown, Massachusetts 02172-0001

The findings in this report are not to be construed as an official Department of the Army position, unless so designated by other authorized documents.

Mention of any trade names or manufacturers in this report shall not be construed as advertising nor as an official indorsement or approval of such products or companies by the United States Government.

DISPOSITION INSTRUCTIONS

Destroy this report when it is no longer needed.
Do not return it to the originator.

UNCLASSIFIED

SECURITY CLASSIFICATION OF THIS PAGE *(When Data Entered)*

REPORT DOCUMENTATION PAGE		READ INSTRUCTIONS BEFORE COMPLETING FORM
1. REPORT NUMBER MTL TR 90-63	2. GOVT ACCESSION NO.	3. RECIPIENT'S CATALOG NUMBER
4. TITLE *(and Subtitle)* A DETERMINATION/VALIDATION OF AUTOCLAVE FORCED CONVECTION HEATING		5. TYPE OF REPORT & PERIOD COVERED Final Report 6. PERFORMING ORG. REPORT NUMBER
7. AUTHOR(s) Steven M. Serabian, and Donald J. Jaklitsch		8. CONTRACT OR GRANT NUMBER(s)
9. PERFORMING ORGANIZATION NAME AND ADDRESS U.S. Army Materials Technology Laboratory Watertown, Massachusetts 02172-0001 SLCMT-MRS		10. PROGRAM ELEMENT, PROJECT, TASK AREA & WORK UNIT NUMBERS D/A Project: IL162105AH84 AMCMS Code: 612105.AH840011
11. CONTROLLING OFFICE NAME AND ADDRESS U.S. Army Laboratory Command 2800 Powder Mill Road Adelphi, Maryland 20783-1145		12. REPORT DATE December 1990 13. NUMBER OF PAGES 21
14. MONITORING AGENCY NAME & ADDRESS *(if different from Controlling Office)*		15. SECURITY CLASS. *(of this report)* Unclassified 15a. DECLASSIFICATION/DOWNGRADING SCHEDULE
16. DISTRIBUTION STATEMENT *(of this Report)* Approved for public release; distribution unlimited.		
17. DISTRIBUTION STATEMENT *(of the abstract entered in Block 20, if different from Report)*		
18. SUPPLEMENTARY NOTES		
19. KEY WORDS *(Continue on reverse side if necessary and identify by block number)* Autoclave Curing Forced convection Slug meter Composites Finite elements Experimental		
20. ABSTRACT *(Continue on reverse side if necessary and identify by block number)* (SEE REVERSE SIDE)		

DD FORM 1 JAN 73 1473 EDITION OF 1 NOV 65 IS OBSOLETE

UNCLASSIFIED

SECURITY CLASSIFICATION OF THIS PAGE *(When Data Entered)*

Block No. 20

ABSTRACT

The top face of a semi-infinite, plaster of paris slab was heated by forced convection in an autoclave while its depthwise temperature profile was obtained as a function of time by embedded thermocouples. The average forced convection heat transfer parameter of the slab's top face was determined from a time dependent lumped parameter analysis of temperature data acquired from two slug meters of varying design. The resulting nonlinear convective boundary conditions were applied to a transient heat transfer model of the semi-infinite slab to predict depthwise temperature profiles as a function of time. The model's thermal property data base was developed using a flash pulse method to determine thermal diffusivity and differential scanning calorimetry (DSC) to determine specific heat. Model temperatures compared poorly to experimental temperatures using the convective boundary condition obtained from the conventional wood slug meter design. However, a 5% temperature comparison was observed using the convective boundary condition obtained from the hybrid cork/fiberglass slug meter design. Finite element heat transfer analysis of the slug meters themselves illustrated the effects of heat retention on slug meter performance.

CONTENTS

INTRODUCTION

Autoclave Curing of Composite Structures

Structural application of polymer based composite materials has risen dramatically in recent years in both defense and commercial markets. Resulting improvements in product design and performance, all but unattainable with conventional materials, are leading to advanced applications with even larger benefits. Some of these benefits, such as the reduced spallation in tanks and the stealthy characteristics in submarines, however, require the use of larger and thicker composite structures. Attempts have been made to reduce the manufacturing costs of these structures by both parts consolidation and the use of co-curing manufacturing methodologies. As these trends continue, cure cycle specification has grown increasingly important to insure manufacturing reliability. Past trial and error methods prove far too costly to be tried with expensive large scale structures.

Considerable effort is presently being expended to try to model the curing of large scale composite structures.[1-3] The effects of autoclave cure cycle parameters such as ramp and dwell times, temperature, and pressure, as well as tool design and placement upon part quality, are being investigated through predictive methods given a characterization of the material's thermal properties and resin kinetics. Numerical simulations which vary these parameters are attempting to define an optimized cure cycle to develop more reliable and less expensive manufacturing processes.

Inherent in this modeling process, among other things, is an estimation of the part's thermal forced convection boundary condition. It is this boundary condition which results in the thermal transport of autoclave energy to initiate and, in some instances, drive the material's matrix chemical reaction that is responsible for curing. Estimation of this time dependent parameter is of prime importance if modeling accuracy is to be achieved. Recent work has attempted to characterize this parameter based on the flow characteristics within the autoclave[2,4] or through the use of slug meter type instrumentation.[5] The simplicity of the latter approach is appealing in light of the level of effort needed to characterize the complicated flow patterns within a fully loaded autoclave. This pointwise determination of the parameter readily lends itself to this situation.

Scope of Work

This effort is an extension of the earlier slug meter approach of Reference 5. It attempts, not only to provide a quantitative validation of the approach, but also to extend it into the nonlinear regime for versatility in future applications. The work attempts to numerically model and validate the forced convection heating of a typical autoclave cure cycle.

1. RAJU, D. S., and MALLOW, A. *Science-Based Guidelines for the Autoclave Process for Composite Manufacturing.* SAMPE Journal, v. 26, no. 3, May-June 1990, p. 31-37.
2. THOMAS, J. A., MALLOW, A. R., MUNCASTER, F. R., HAHN, G. L., CAMPBELL, F. C., McCARVILL, W. T., and BROCKMAN, R. A. *Computer-Aided Curing of Composites.* Materials Laboratory (WRDC/MBLBC), Report No. WRDC-TR-89-4084, Wright-Patterson, AFB, OH, October 1989.
3. BOGETTI, T. A., and GILLESPIE, J. W., Jr. *Processed-Induced Stress and Deformation in Thick-Section Thermosetting Composite Laminates.* 21st SAMPE Technical Conference, Atlantic City, NJ, September 25-28, 1989.
4. GHARIBAN, N. S., HAJI-SHEIKH, A., and LOU, D. Y. S. *Heat Transfer in Autoclaves.* University of Texas at Arlington. To be published.
5. PURSLEY, M. D. *Cure Cycle Definition Methodology for Thick Sectioned Thermosetting Resin Laminates.* Thirty-Sixth Sagamore Army Materials Research Conference, Plymouth, MA, October 23-26, 1989.

A simplified, isotropic, semi-infinite slab configuration has been chosen to reduce modeling complexities and isolate key experimental concerns. Experimental determination of the slab's time dependent, depthwise temperature profile and forced convection heat transfer parameter will be undertaken. Numerical simulation of this heat transfer process using the experimental forced convection boundary condition will be performed and the results compared with the slab's experimental temperature distribution to validate all experimental procedures and hardware used. It is hoped that both the experimental approach and hardware design employed in this report will be used to investigate the autoclave curing of more complicated structures manufactured from advanced composite materials.

FORCED CONVECTION HEATING OF A SEMI-INFINITE PLASTER OF PARIS SLAB

A plaster of paris slab with embedded thermocouples was manufactured and heated on its top surface by the forced convection heating of an autoclave. Embedded thermocouples monitored interior slab temperatures. The slab's top face convective boundary condition was estimated from the temperature data acquired from two slug meters of different design.

Experimental Arrangement

A 12 x 12 x 4 inch inner dimension wooden frame, coated with Carnauba wax, was clamped to a plywood base plate that was covered with a release film. Six J-type (20 AWG) thermocouples were located at approximately 0.125, 0.250, 0.50, 0.75, 1.00, and 1.50 inch depths from the bottom plywood plate by suspending them from above with a metal rod that was laid across the top of the wooden frame. Durabond plaster of paris was mixed in a two-to-one ratio with tap water and poured into the mold. The top surface of this three inch deep form was leveled with a ruler avoiding disturbance of the thermocouple wires. After a 24-hour cure period, the plaster slab was removed from its wooden mold. The slab was radiographed to locate actual thermocouple positions to reduce any associated experimental error. Actual thermocouple depths were 0.175, 0.340, 0.550, 0.910, 1.240, and 1.710 inch.

A 2.5 x 3.5 foot wooden frame manufactured from 2 x 4 inch stock was covered with 0.5-inch-thick plywood sheeting. From this sheeting, a central opening was cut with dimensions approximately equal to those of the plaster slab. Internal 2 x 4 inch crossbracing was added at equal distances from this opening and each end of the frame. These areas were filled with fiberglass insulation. The initial slug meter design consisted of two thin 6061-T6 aluminum plates measuring 2 x 1 x 0.125 inch which were instrumented with J-type (36 AWG) thermocouples and countersunk into the plywood top of the wooden frame to the left and right of the slab.

The wooden frame was placed over the plaster slab carefully aligning its central cutout exposing the slab's top surface. A J-type (36 AWG) thermocouple was attached to the bottom surface of the slab with high temperature adhesive tape. A thick layer of fiberglass insulation was placed underneath the slab to raise its top surface to that of the wooden frame. Stiffer J-type (20 AWG) thermocouples were affixed approximately two inches above the central region of the aluminum plates by prebending and stapling them to the plywood.

The entire assembly, as shown in Figure 1, was placed into a three foot diameter by six foot length autoclave manufactured by Devine. All 10 thermocouple ends were connected to ceramic plugs within the autoclave. Intermediate wires were run from these plugs into a Cyborg data acquisition system. Thermocouple readings from the plaster slab, aluminum

plates, and stagnant air were allowed to reach room temperature equilibrium prior to sealing of the autoclave door and ensuing heating procedures.

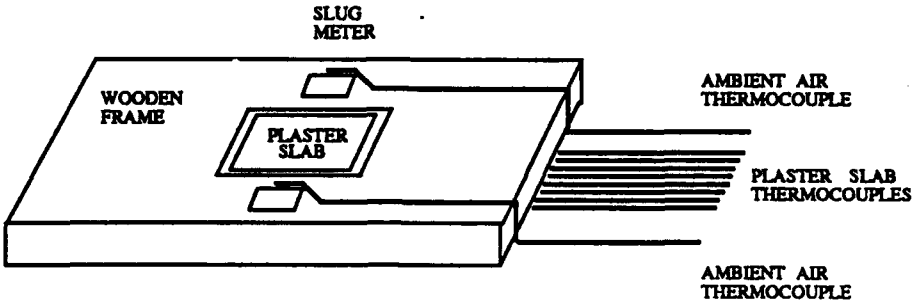

Figure 1. Semi-infinite plaster slab experimental arrangement.

Experimental Procedures

Thermocouple temperature readings were acquired by the data acquisition system at a rate of one sample every two seconds. After approximately one minute of room temperature readings, the autoclave blower and heat elements were activated. The autoclave was ramped up to a temperature of 400°F by using the maximum available heating rate. Temperature readings were recorded by the data acquisition system until maximum autoclave temperatures were reached. At such time, the heater element was shut off and the slab was cooled by using the blower in conjunction with the autoclave's cooling coils. Temperature data files were written to floppy disk and uploaded to an Apollo Domain Series 2500 Work Station by way of a file transfer process. File results were displayed using *PATRAN'S XY* Plotting Package.

EXPERIMENTAL DETERMINATION OF AUTOCLAVE FORCED CONVECTION HEATING

A lumped parameter analysis of the slug meter temperature data was done to calculate the forced convection heat transfer parameter. These calculations were done at each temperature-time data point after steady state-plate heating was achieved. Results indicated a nonlinear decrease of the parameter with increasing time.

Transient Lumped Parameter Slug Meter Data Analysis

The dimensional characteristics and material selection of the plates used in the slug meters were selected in conjunction with an initial estimation of the forced convection boundary condition. Both the plate's thermal conductivity (k_p) and thickness (t) were selected to insure an appreciable difference between its internal conductive and surface convective resistances. A low value of this ratio, which is more commonly known as the Biot number, insured a near uniform temperature distribution throughout the plate.[6] This distribution allowed for a simplified lumped parameter analysis of the plate to obtain the forced convection heat transfer coefficient (h).

6. HOLMAN, J. P. *Heat Transfer*. Fourth Edition, McGraw-Hill, New York, NY, 1976.

By performing an energy balance on the plate and assuming that all energy from its convective heating is used to increase its internal energy, the following relationship was obtained:[7]

$$h\ A\ \Delta T = m\ (\partial T/\partial t)\ C_P \qquad (1)$$

where

h	=	convective heat transfer coefficient
A	=	exposed plate area
ΔT	=	plate and ambient air temp. difference
m	=	plate mass
C_P	=	plate specific heat
$\partial T/\partial t$	=	plate temp. change rate

Solving for the convective coefficient;

$$h = \frac{m\,(\partial T/\partial t)}{A\,\Delta T} C_P \qquad (2)$$

Figure 2 shows the left and right slug meter and ambient air temperature-time results. As was expected, slug meter temperatures lagged behind ambient air temperatures. Little variation was seen between left- and right-hand sides. The maximum heat ramp rate of the autoclave produced nonlinear ambient air temperature profiles. Boiling and evacuation of residual cooling coil water was responsible for the observable hump in this data. Slug meter temperatures appeared to rise linearly after initial nonlinear behavior.

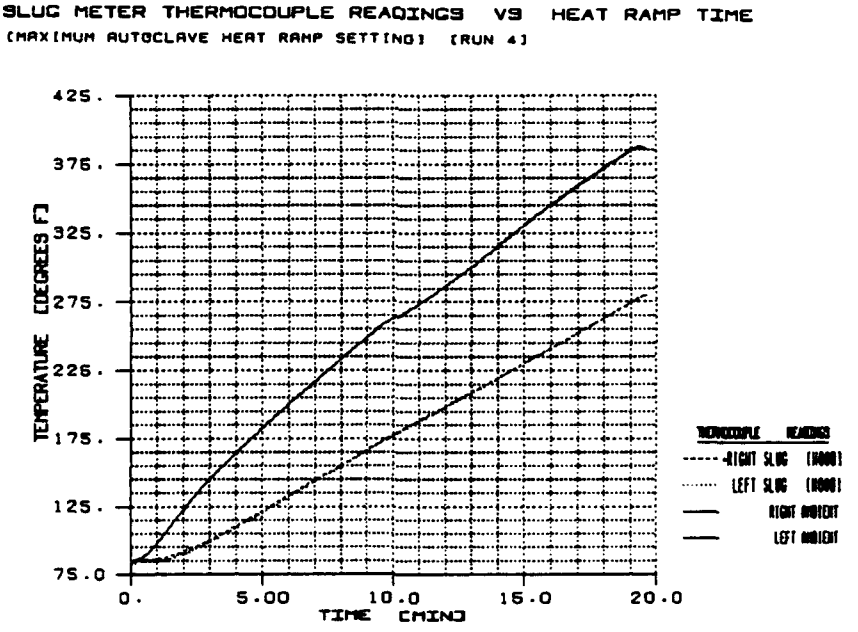

Figure 2. Slug meter thermocouple readings versus heat ramp time.

7. PITTS, D. R., and SISSON, L. E. *Theory and Problems of Heat Transfer*. McGraw-Hill, New York, NY, 1977.

Also as shown in Figure 2, both the plate temperature change rate ($\partial T/\partial t$) and the temperature difference between the plate and ambient air (ΔT) were a function of time and, thus, not constant. Furthermore, zero ΔT and $\partial T/\partial t$ values were observed at the onset of heating. These characteristics in the temperature data suggested a nonlinear convection coefficient whose intial value was undefined.

Meaningful values of the convection coefficient were obtained by applying Equation 2 in a transient fashion after steady state heating of the plate presented itself. Calculations at each time period of the temperature data files were made after steady state plate heating was achieved. Plate temperature change rates were smoothed by averaging each temperature reading with its three prior and subsequent values.

Experimental Results

Figures 3 and 4 illustrate the forced convection coefficient values resulting from the calculations of Equation 2. As might be anticipated from the temperature histories shown in Figure 2, there was no apparent variation between the coefficients obtained for the left and right slug meters. This data was fit with a third order least squares curve fit whose form is shown in Equation 3 and whose constants are listed in Table 1. In a similar fashion, autoclave ambient air temperature data was also curve fit. Their constants may be seen in Table 2.

$$h(t) = C_o + C_1 t + C_2 t^2 + C_3 t^3 \qquad (3)$$

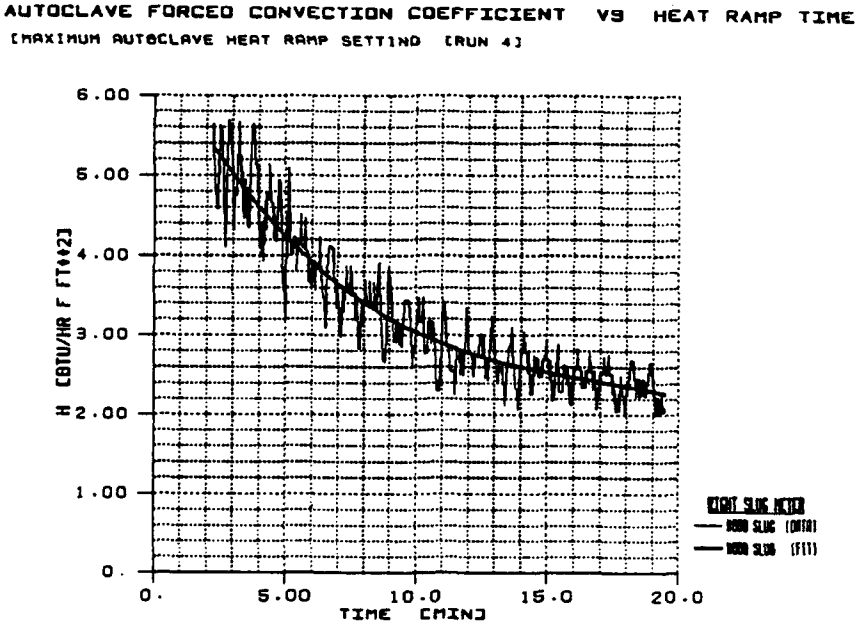

Figure 3. Autoclave forced convection coefficient versus heat ramp time (right slug meter).

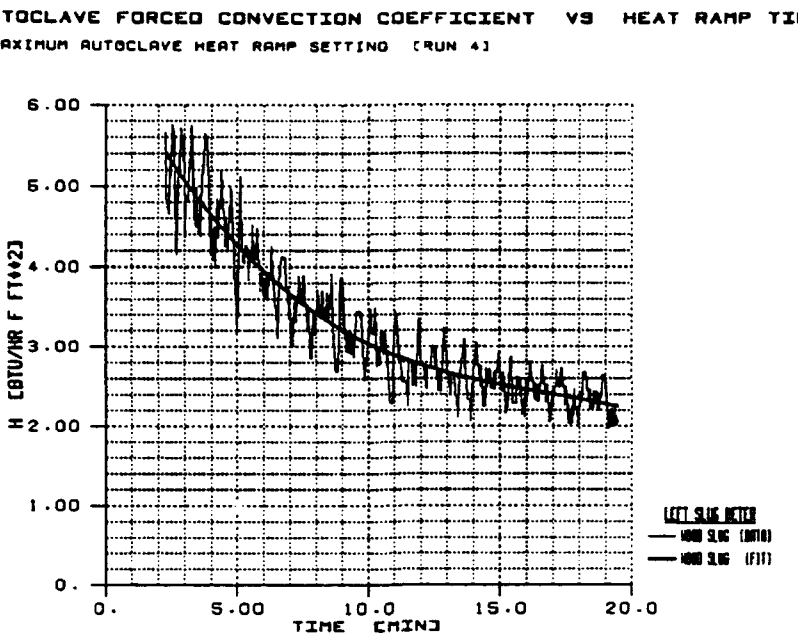

Figure 4. Autoclave forced convection coefficient versus heat ramp time (left slug meter).

Table 1. AUTOCLAVE FORCED CONVECTION LEAST SQUARES CURVE FIT CONSTANTS

	Least Squares Curve Fit Constants			
Slug Meter	C_o	C_1	C_2	C_3
Left	6.706E+06	-6.439E+05	3.450E+04	-6.769E+02
Right	6.622E+06	-6.290E+05	3.336E+04	-6.576E+02

Table 2. AUTOCLAVE AMBIENT AIR TEMPERATURE LEAST SQUARES CURVE FIT CONSTANTS

	Least Squares Curve Fit Constants			
	C_o	C_1	C_2	C_3
Ambient Air	7.890E+01	2.987E+01	-1.291E+00	3.598E-02

TRANSIENT HEAT TRANSFER ANALYSIS OF A SEMI-INFINITE PLASTER OF PARIS SLAB

In an attempt to validate the experimental forced convection heat transfer parameter, the boundary condition was applied to a semi-infinite plaster slab finite element model. Temperature predictions were obtained at seven time intervals during slab heating. Material properties for the model were obtained by flash pulse and differential scanning calorimetry (DSC) methodologies.

Finite Element Model

A finite element model of the plaster slab was assembled using the commercially available code *ABAQUS*. A total of 20 DC2D8 planar heat transfer elements were used to construct the model. The eight-node, quadratic interpolation function elements were arranged in a coarse to fine mesh gradation in anticipation of the slab's temperature profile. As shown in Figure 5, the model was three inch in length with the largest and smallest element length being 0.45 inch and 0.05 inch, respectively.

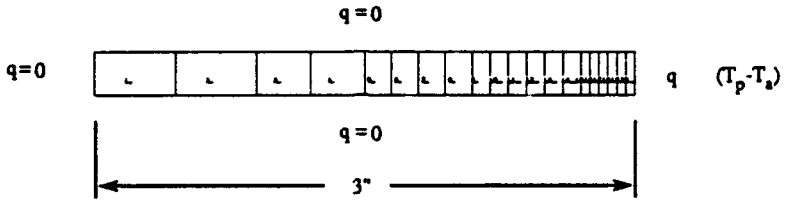

Figure 5. Semi-infinite plaster slab finite element model.

The model was loaded with the nonlinear forced convection boundary condition at the fine mesh end while all remaining three sides were thermally insulated with a zero flux boundary condition. A user defined subroutine was written to apply the convective boundary condition. The subroutine calculated both the forced convection boundary condition and ambient air sink temperature as a function of time. The least squares curve fit constants of Table 1 and Table 2 were used in these subroutine calculations.

Thermal Property Data Base

A thermal property data base consisting of specific heat, thermal conductivity, and density was generated for the plaster material and used in the material description section of the *ABAQUS* input deck. DSC was used to obtain specific heat measurements while water displacement was used to obtain density measurements. The flash pulse method was employed to measure thermal diffusivity. Thermal conductivity was calculated from thermal diffusivity, specific heat, and density values. All measurements were made at room temperature. All properties of the thermal data base were assumed to be independent of temperature for the temperature range under consideration.

Specific heat (C_p) measurements were made with a Perkin-Elmer, model DSC-2, differential scanning calorimeter. The instrument is used to obtain a comparative measurement of the amount of heat needed to raise the temperature of a sample material at a set rate. Within the instrument, two identical calorimeters are instrumented to operate at the same temperature and are programmed to increase temperature at the same rate.[8] A piece of the sample material of unknown specific heat is placed in the pan of one calorimeter while the other calorimeter is left empty. The difference in electrical power needed to maintain identical pan temperatures during heatup is measured. Comparisons to similarly obtained values from a reference material with known specific heat yields specific heat values of the sample material. Adjustments to this specific heat value due to thermoelectric variations between calorimeters are estimated by measuring electrical power differences between the calorimeters themselves during heatup (i.e., no samples).

8. BAIJAL, MAHENDRA. *Plastics and Polymer Science and Technology*. John Wiley & Sons, New York, NY 1982, p. 856.

All DSC scans were run from 310 K to 330 K at a 10 degree/minute heatup rate. A synthetic sapphire aluminum oxide was used as the reference material. Three separate scans were run for each of the preweighed plaster and sapphire samples. Three separate scans were also run using empty pans. Electrical power amplitude measurements (A_i) were made from each scan at 320 K from DSC graphic output, which is shown in typical form in Figure 6. In calculating the specific heat of the plaster, average peak amplitudes (A_{ave}) and specimen weights ($W_{ref\ ave}$ and $W_{pl\ ave}$) were used in accordance to the following relationship.

$$C_{p\,pl} = \frac{A_{pl\,ave} \pm A_{pan\,ave}}{A_{ref\,ave} \pm A_{pan\,ave}} \frac{W_{ref\,ave}}{W_{plf\,ave}} C_{p\,ref} \qquad (4)$$

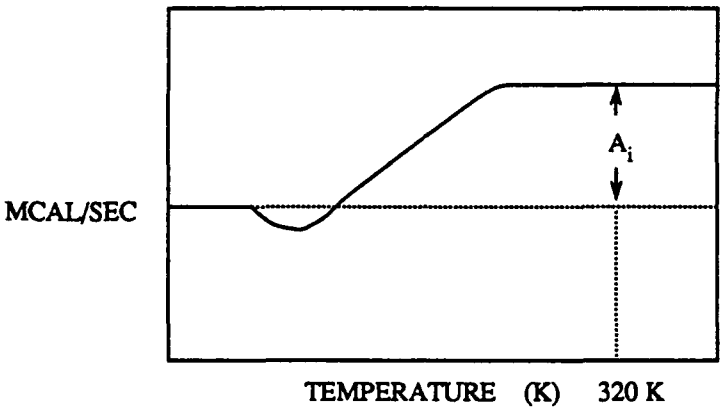

Figure 6. Amplitude determination of typical DSC scan.

The density of the plaster material (ρ_{pl}) was determined using a pyknometer. This instrument was used to measure the weight of water displaced by a plaster sample. From this weight, the sample's volume was determined and was used to calculate its density. A total of five samples were used for these determinations. Weight measurements of the plaster samples were made after immersion and compared to those made prior to immersion to insure that water uptake did not occur.

The plaster's thermal conductivity (K_{pl}) was obtained indirectly from the materials thermal diffusivity (α_{pl}) which is related to specific heat and density by the following relationship:

$$\alpha_{pl} = \frac{K_{pl}}{\rho_{pl} C_{p\,pl}} \qquad (5)$$

A flash pulse method was used to measure the plaster's thermal diffusivity.[9] In this method, a sample is irradiated by a short pulse of energy that is assumed to be instantaneously absorbed at the sample's surface. Assuming that the sample's diffusivity remains constant over its temperature change and that no phase change or heat loss occurs, a trace of the sample's back surface temperature rise may be used to graphically determine its diffusivity.

9. JENKINS, R. J., and PARKER, W. J. *Flash Method of Determining Thermal Diffusivity, Heat Capacity, and Thermal Conductivity.* WADD Technical Report No. 61-95, U.S.N. Rad. Def. Lab., Project No. 7360, June 1961, p. 1-25.

All of these assumptions may be met by experimentally limiting the energy of the heat pulse such that the maximum back surface temperature rise is a few degrees centigrade. The governing relationship is given by;

$$\alpha = \frac{1.38 L^2}{\pi^2 t_{0.5}} \tag{6}$$

where;

L = sample thickness
$t_{0.5}$ = time to reach half of back surface maximum temperature

The experimental arrangement used for the diffusivity measurements, as shown in Figure 7, consisted of an Ascorlight, Model No. QC8, xenon flash tube, a lexan sample holder, a spring-loaded chromel-alumel thermocouple, a 5000 series Tektronics storage oscilloscope, a Hewlett-Packard X-Y Recorder, and a five-volt power supply. During normal operation, firing of the flash tube triggered the power supply and oscilloscope creating a reference step change that was recorded by the oscilloscope. Output from the open junction thermocouple, which was kept in contact with the back surface of the specimen, was recorded by the oscilloscope. The temperature scan and reference wave form were digitized by the wave form digitizer of the oscilloscope and output to the X-Y recorder for graphic display. Typical display results may be seen in Figure 8.

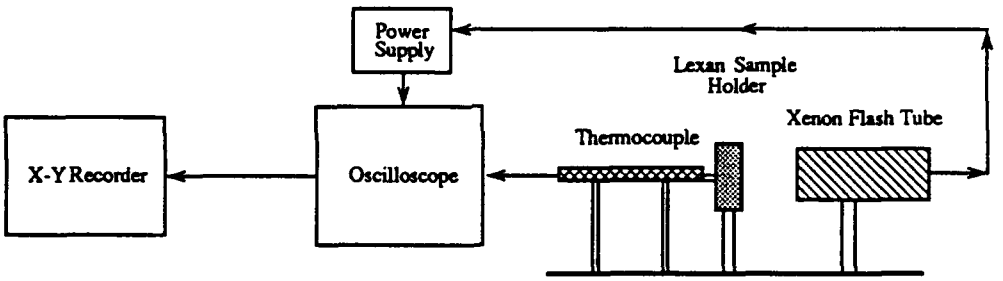

Figure 7. Flash pulse experimental arrangement.

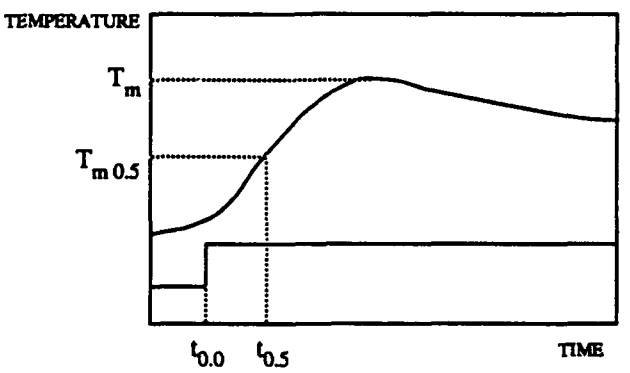

Figure 8. Flash pulse temperature oscilloscope trace.

A total of four 0.75 x 0.75 inch plaster samples were cast and sanded to uniform thickness using a glass plate and 320 grit sandpaper. Thickness measurements, which ranged from 0.062 to 0.188 inches, were made to within a 0.001 inch with a vernier caliper. The samples were coated with a thin layer of a carbon black paste mixture (50 parts carbon black, 25 parts carboxymethylcellulose binder, and 25 parts tetrasodiumpyrophosate) to insure uniform heat absorption. An additional layer of conductive silver paint was applied to the back surface of the samples to promote good electrical contact between the thermocouple and the sample. Care was taken to avoid coating the edges of the sample with this paint thus eliminating any alternate paths for the heat pulse. A total of 17 diffusivity measurements were made between the four specimens.

Average and standard deviation values for specific heat, density, and diffusivity were calculated from all measured results. A conductivity value was obtained from these results and Equation 5. Experimental uncertainty in this value was found from Equation 5 and an uncertainty analysis based on the following equation.[10] Table 3 lists these results.

$$W_k = \{[(\partial K/\partial \alpha)\, W_\alpha]^2 + [(\partial K/\partial \rho)\, W_\rho]^2 + [(\partial K/\partial C_p)\, W_{Cp}]^2\}^{0.5} \qquad (7)$$

where

W_k = conductivity experimental uncertainty
W_α = diffusivity experimental uncertainty
W_ρ = density experimental uncertainty
W_{Cp} = specific heat experimental uncertainty

Table 3. PLASTER OF PARIS THERMAL PROPERTY DATA BASE

Units	Average	Standard Dev.	Exper. Uncert.
C_p (Btu/lb °F)	2.50E-01	3.15E-03	
ρ (lb/in.^{3})	7.60E-02	3.76E-03	
α (in.^{2}/sec)	5.92E-04	6.10E-05	
K (Btu/in. °F min.)	6.74E-04		7.75E-05

Finite Element Computations

All nodal temperatures of the plaster slab finite element model were fixed at the room temperature value that was recorded prior to heating of the actual plaster slab. The convective boundary condition was applied to the finite element model in a total of seven separate steps whose physical time values were 0.5, 1, 2, 4, 8, 13, and 19 minutes, respectively. The transient analysis was run using a fixed number of time increments (10) for each step. The

10. HOLMAN, J. P. *Experimental Methods for Engineers*. Fifth Edition, McGraw-Hill, New York, NY 1989.

number of increments in each step was chosen to eliminate spurious solution oscillations, thus insuring the stability of the finite element code's unconditionally stable backwards difference time integration.[11] The following relationship between the maximum usable time increment and the minimum element size was employed as suggested by *ABAQUS*.[11]

$$\Delta t = \frac{\rho C_p}{6K} \Delta l^2 \qquad (8)$$

where;

Δt = maximum time increment
ρ = density
X_p = specific heat
K = thermal conductivity
Δl^2 = minimum element length

Iteration and convergence within each increment was controlled by a temperature tolerancing parameter (TEMTOL). Correction to the temperature solution at each iteration was required to fall below this parameter for solution acceptance. As suggested by *ABAQUS*, this parameter was set to 1% of the expected temperature changes per increment.[11] Table 4 illustrates a summary of these parameters.

Table 4. TRANSIENT HEAT TRANSFER COMPUTATIONAL PARAMETERS

Step Time (min)	# of Inc	Time/Inc (min)	Temp Tol (°F)	Max ΔT/ Inc (°F)
0.5	10	5E-02	5.0E-04	0.012
1.0	10	5E-02	1.5E-03	0.175
2.0	10	1E-01	3.5E-03	0.609
4.0	10	2E-01	7.0E-03	1.560
8.0	10	4E-01	1.0E-02	3.240
13.0	10	5E-01	1.0E-02	4.940
19.0	10	6E-01	1.0E-02	6.920

EXPERIMENTAL/NUMERICAL COMPARISONS

Comparisons between the plaster slab finite element and experimental results may be seen in Figure 9. It is noted that the finite element temperatures fell well below experimental thermocouple readings. This discrepancy increased with heat ramp time. A series of additional finite element runs were made with separate alterations in thermal conductivity and the

11. HIBBITT, KARLSSON, and SORENSEN. Abaqus Theory Manual (Version 4.8). Hibbitt, Karlsson, and Sorensen Inc., Providence, Rhode Island.

forced convection boundary condition in an attempt to computationally uncover the reason(s) for this poor comparison. Thermal conductivity variations indicated that maximum slab experimental temperatures could be approximated but only by using a conductivity value that was a full order of magnitude lower than that obtained experimentally. In this instance, interior FEA temperatures were increasingly overestimated at longer heating times. However, a doubling of the model's convective heat transfer parameter yielded entire temperature profiles that were within 20% throughout the entire heating process. This latter observation raised questions regarding the validity of the experimentally obtained heat transfer parameter.

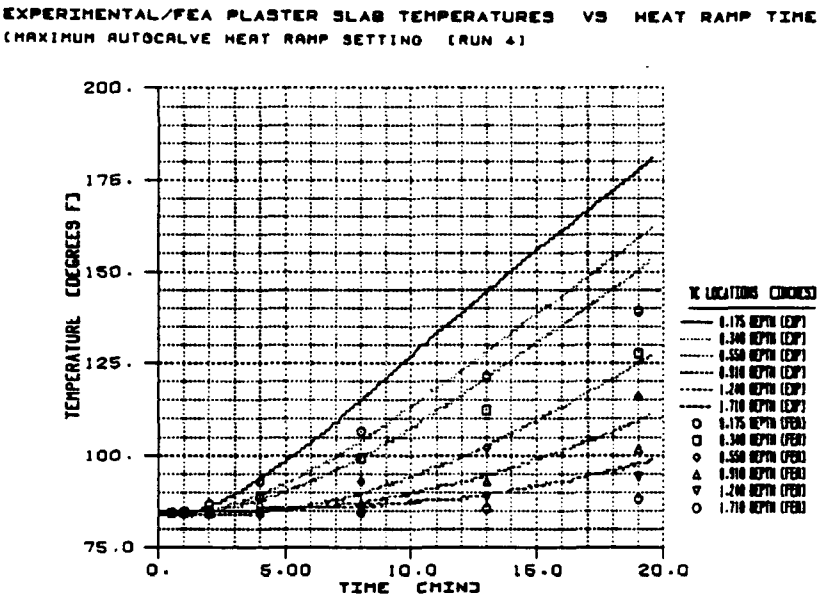

Figure 9. Experimental/numerical plaster slab temperature comparisons.

INSTRUMENTATION IMPROVEMENTS

A thermal finite element analysis of the initial slug meter was conducted to qualify its ability to accurately determine the convection coefficient. Based upon these results, a new hybrid slug meter was designed using granulated cork and fiberglass. Original plate temperatures that were used to define the convection parameter were recovered in a thermal finite element analysis of this hybrid design, thus signifying its adequacy.

Slug Meter Thermal Analysis

A two-dimensional transient heat transfer analysis of the aluminum/wood slug meter was undertaken to evaluate its ability to accurately estimate the forced convection boundary condition. The model was constructed in *ABAQUS* using 180 of the same elements previously used in the plaster slab model. The half symmetry model was insulated with a zero flux boundary condition on all but the top surface where the experimental convective boundary condition was applied, as shown in Figure 10. Handbook values of thermal conductivity, specific heat, and density for the aluminum and wood (Douglas Fir) model materials were used.[6] Finite element computations were handled in a fashion similar to that of the plaster slab with appropriate changes in the maximum permissible time increment in accordance with Equation 6.

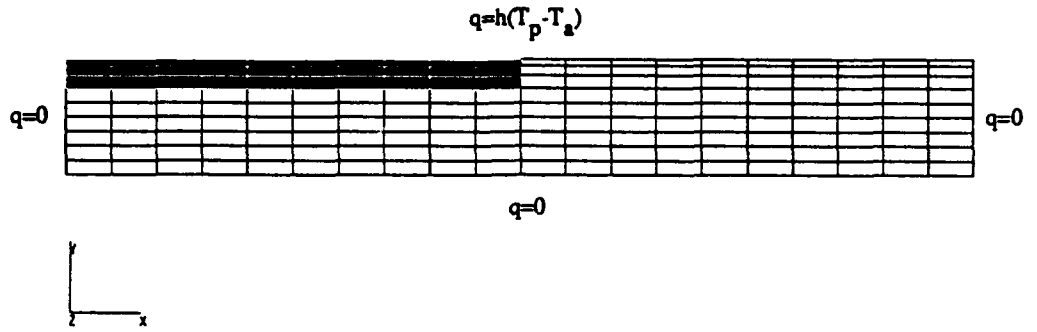

Figure 10. Two-dimensional aluminum/wood slug meter finite element model.

Comparisons between analysis results for the last time step, as shown in Figure 11, and experimental results of Figure 2, clearly illustrated significantly lower aluminum plate FEA temperatures. The inability to computationally recover experimental plate temperatures, from which the convective boundary condition was derived, indicated a violation of the heat transfer assumption on which the lumped parameter analysis was based. Significant heat flow from the aluminum plate, which occurred due to the poor insulating characteristics of the wood backing plate, acted to lower FEA plate temperatures. As can be seen by Equation 2, lower plate temperatures (increased ΔT) reduce the calculated value of the convective heat transfer parameter. The aluminum/wood slug meter design, thus, underestimated the convective heat transfer parameter.

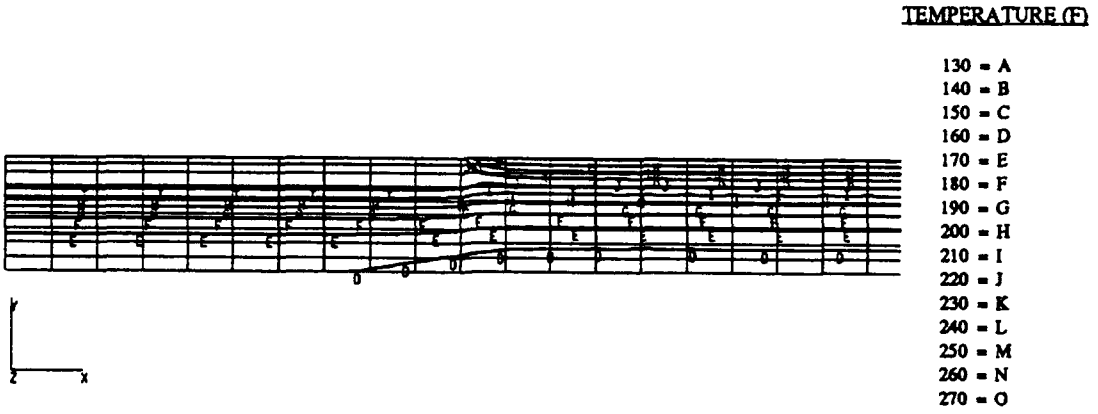

Figure 11. Two-dimensional aluminum/wood slug meter finite element results.

Slug Meter Redesign

In an effort to reduce detrimental heat flow from the aluminum plate, a hybrid slug meter was designed and numerically evaluated using finite element approximations. The wood backing was replaced with a thicker cork/fiberglass combination, as shown in Figure 12. The increased thickness and use of materials, whose thermal conductivities were approximately 2.5 to 3 times lower than that of the wood, were thought to provide a better thermal barrier to retain the heat of the aluminum plate.

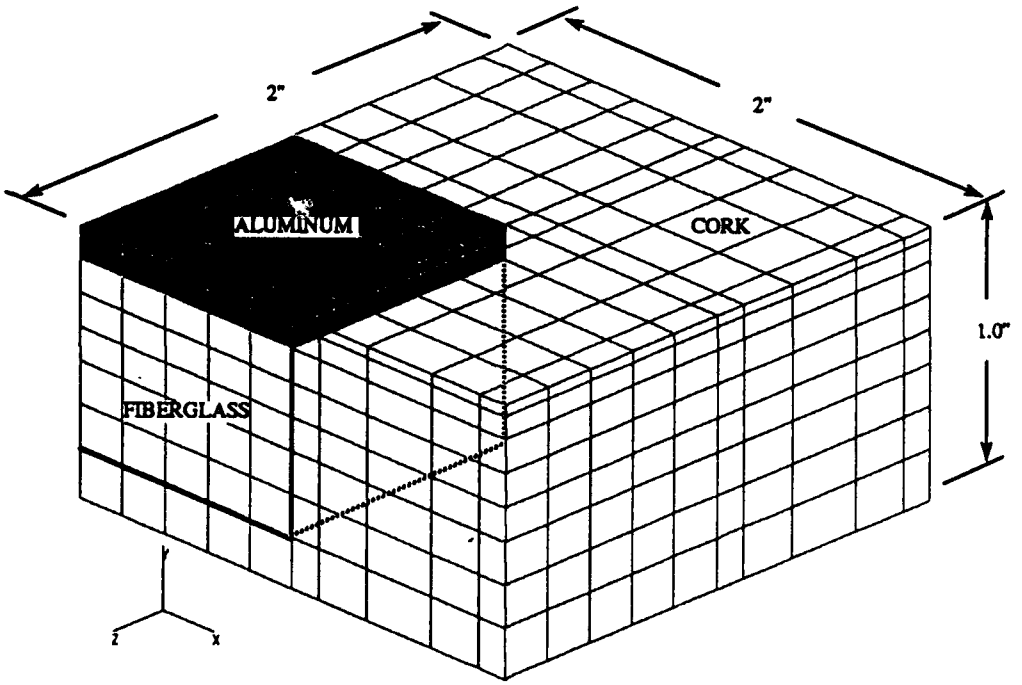

Figure 12. Three-dimensional hybrid slug meter finite element model.

A quarter symmetry finite element model of the hybrid slug meter was constructed using a total of 800 DC3D20, quadratic interpolation, *ABAQUS* heat transfer elements. The convective boundary condition was applied to the top and two outer sides while the bottom and two inner sides were insulated. Discretization was performed to accommodate heat flow from all convective surfaces, as well as heat flow between the aluminum plate and the cork backing material. As was the case for all other computations, a total of seven steps were used in the analysis and appropriate increment times (in accordance with the minimum element length) were used to avoid solution instability.

Analysis results indicated reduced heat flow from the aluminum plate and recovery of actual experimental plate temperatures within 2%. These results, which adhered to the heat transfer assumptions of the lumped parameter analysis, clearly demonstrated the superiority and qualification of the hybrid slug meter design. Figure 13 illustrates last step temperature profiles of the hybrid design while Table 5 summarizes experimental plate temperatures and analysis results for both slug meter designs.

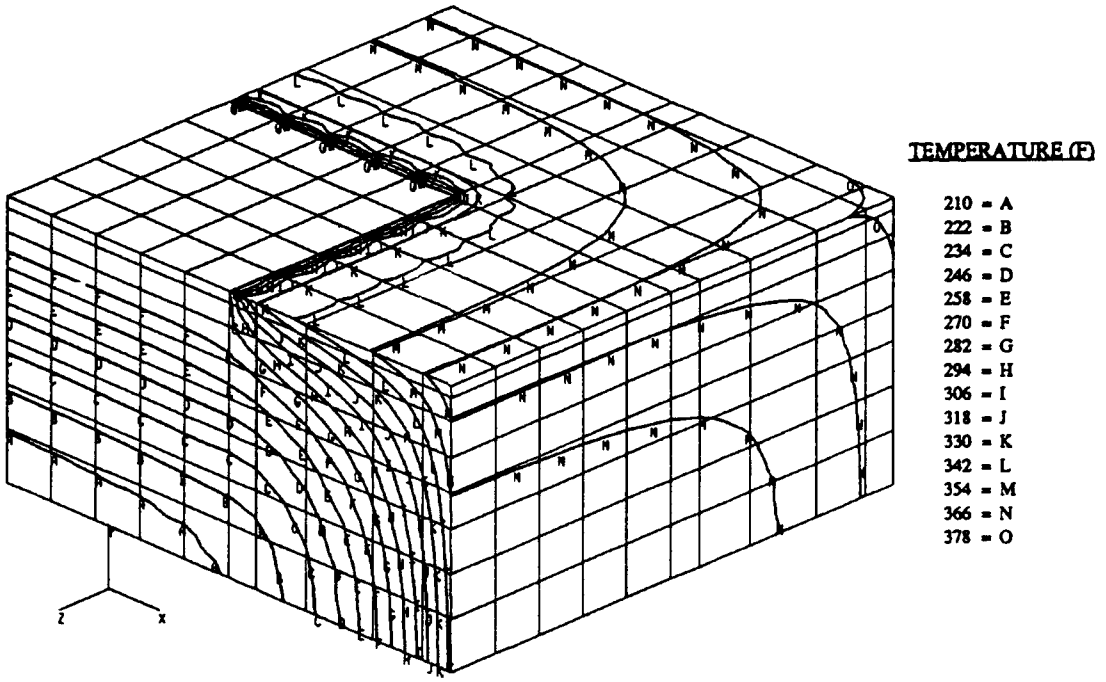

Figure 13. Three-dimensional hybrid slug meter finite element results.

Table 5. SLUG METER FINITE ELEMENT ANALYSIS RESULTS

Time Step	Time (min)	Exp. Plate Temp. (°F)	FEA Plate Temp. (°F) Cork/Fiberglass	FEA Plate Temp. (°F) Plywood
1	0.5	85	84.78	84.85
2	1.0	87	88.18	85.99
3	2.0	91	92.44	90.68
4	4.0	111	112.00	104.40
5	8.0	155	157.50	134.40
6	13.0	210	212.00	169.70
7	19.0	275	277.40	213.30

IMPROVED EXPERIMENTAL/NUMERICAL DETERMINATIONS

A slug meter of the hybrid design was manufactured by adhering several layers of precut granulated cork sheets with contact cement. Glass wool fiberglass was packed into the central cavity of the cork square and the aluminum plate/thermocouple assembly was fit on top. Autoclave heating of the plaster slab was carried out again using both types of slug meters to estimate the forced convection heat transfer parameter. Slug meter temperature data was processed as before. Figure 14 illustrates the slug meter data, while Figure 15 shows the resulting forced convection parameter for each slug meter design. As can be seen, higher plate temperatures were observed for the hybrid slug meter design indicating increased thermal insulation from the cork and fiberglass materials. These increased plate temperatures resulted in a more than twofold increase in the forced convection parameter, as indicated in Figure 15.

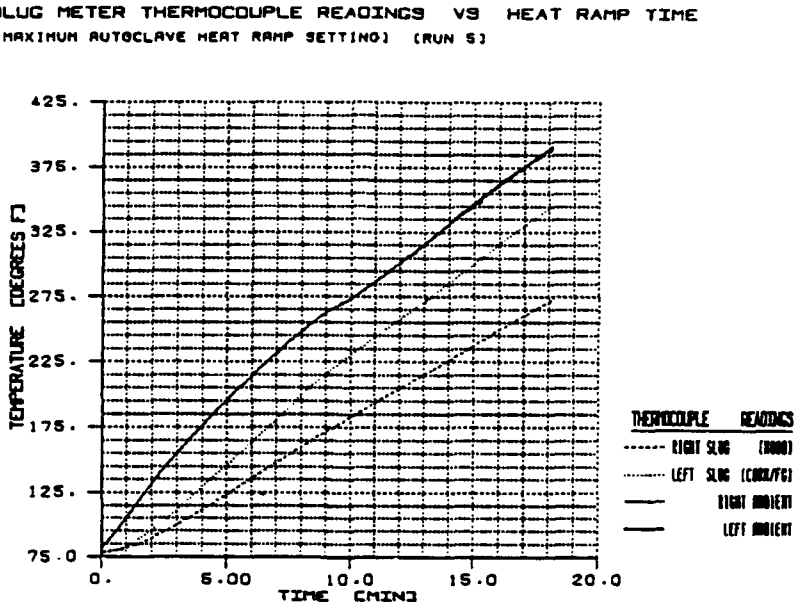

Figure 14. Conventional/hybrid slug meter thermocouple temperature readings.

The finite element model of the semi-infinite plaster slab was run again with a curve fit representation of the larger forced convection boundary condition. Figure 16 illustrates a comparison between resulting model temperatures and experimental results. As can be seen, a close correlation was observed indicating the accuracy of the experimentally determined autoclave convective boundary condition.

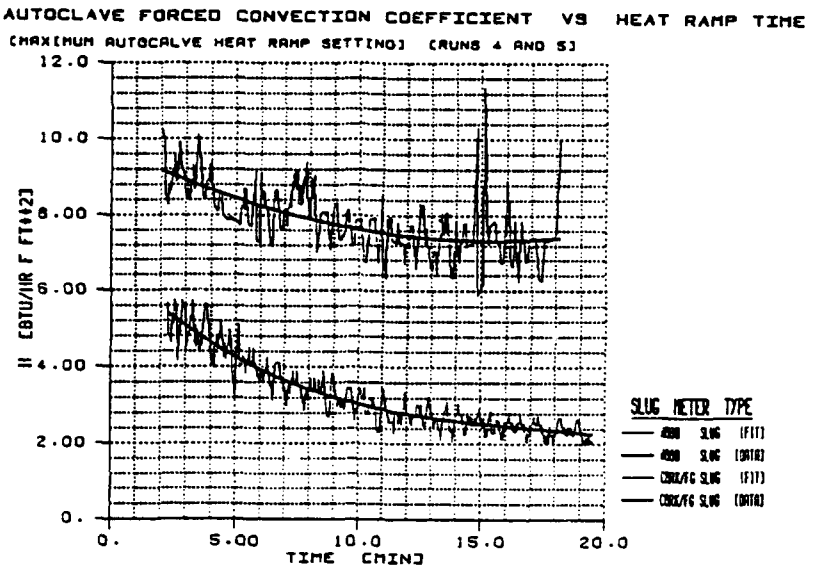

Figure 15. Forced convection coefficient for wood and cork/fiberglass slug meters.

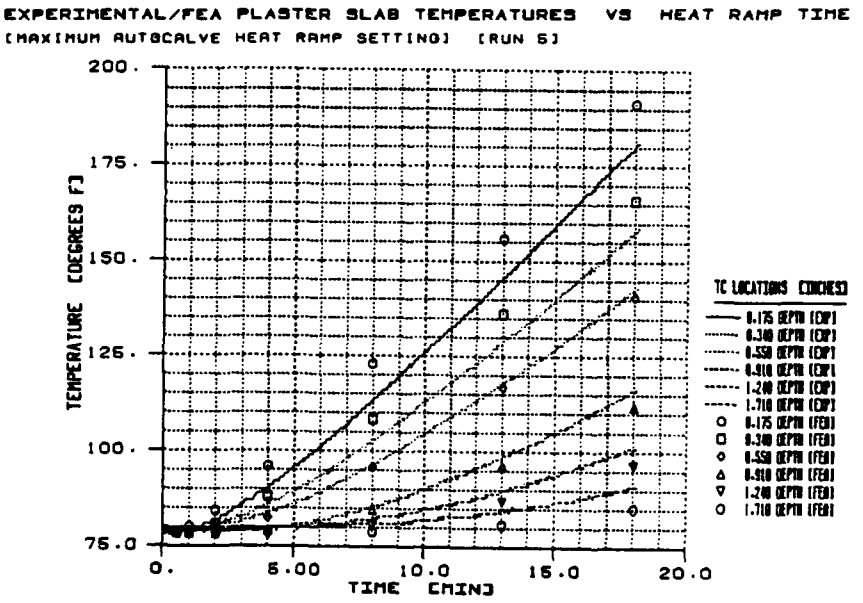

Figure 16. Improved experimental/numerical plaster slab temperature comparisons.

CONCLUSIONS

The forced convection heat transfer parameter of a typical autoclave heat ramp has been obtained experimentally. An improved hybrid slug meter, whose design concept was qualified through a thermal finite element analysis, determined this parameter precisely while a conventional wood based slug meter underestimated it by more than a factor of two. A numerical representation of the correct parameter was used in a transient finite element heat transfer analysis of a semi-infinite plaster slab whose thermal properties were determined from flash pulse and DSC methodologies. Finite element depthwise temperature profiles as a function of time were within 5% agreement with experimental temperature profiles obtained from a plaster slab with embedded thermocouples under the same convective heating conditions.

RECOMMENDATIONS FOR FUTURE WORK

The convective heat transfer parameter during the remaining temperature dwell and cooling periods of a typical autoclave cure cycle could also be obtained using the hybrid slug meter design and experimental/analytical procedures detailed in this report. Furthermore, a "mapping" of this parameter throughout the autoclave should be done since nonuniform flow and extreme turbulence conditions present themselves. This full field, total cure cycle convective heat transfer parameter could be applied to the modeling efforts of more complicated, large scale, thick composite structures. Improved tool thermal designs, autoclave loading schemes, and new efficient cure cycles could be defined resulting in lower energy costs and improved part quality.

ACKNOWLEDGMENTS

The authors would like to thank Dr. John Quigley of the Concurrent Engineering Directorate at AMC for his financial assistance, Mr. Shawn M. Walsh for his valuable insight in slug meter instrumentation, Mr. William Green and Mr. Thomas Harkins for their radiographic work, Dr. J. Walkinshaw for his suggestions regarding model material suggestions, and Ms. Maria Bostic for her software assistance.

DISTRIBUTION LIST

No. of Copies	To
1	Office of the Under Secretary of Defense for Research and Engineering, The Pentagon, Washington, DC 20301
	Commander, U.S. Army Laboratory Command, 2800 Powder Mill Road, Adelphi, MD 20783-1145
1	ATTN: AMSLC-IM-TL
1	AMSLC-CT
	Commander, Defense Technical Information Center, Cameron Station, Building 5, 5010 Duke Street, Alexandria, VA 22304-6145
2	ATTN: DTIC-FDAC
1	Metals and Ceramics Information Center, Battelle Columbus Laboratories, 505 King Avenue, Columbus, OH 43201
	Commander, Army Research Office, P.O. Box 12211, Research Triangle Park, NC 27709-2211
1	ATTN: Information Processing Office
	Commander, U.S. Army Materiel Command, 5001 Eisenhower Avenue, Alexandria, VA 22333
1	ATTN: AMCLO
	Commander, U.S. Army Materiel Systems Analysis Activity, Aberdeen Proving Ground, MD 21005
1	ATTN: AMXSY-MP, H. Cohen
	Commander, U.S. Army Missile Command, Redstone Scientific Information Center, Redstone Arsenal, AL 35898-5241
1	ATTN: AMSMI-RD-CS-R/Doc
1	AMSMI-RLM
	Commander, U.S. Army Armament, Munitions and Chemical Command, Dover, NJ 07801
2	ATTN: Technical Library
1	AMDAR-LCA, Mr. Harry E. Pebly, Jr., PLASTEC, Director
	Commander, U.S. Army Natick Research, Development and Engineering Center, Natick, MA 01760-5010
1	ATTN: Technical Library
	Commander, U.S. Army Satellite Communications Agency, Fort Monmouth, NJ 07703
1	ATTN: Technical Document Center
	Commander, U.S. Army Tank-Automotive Command, Warren, MI 48397-5000
1	ATTN: AMSTA-ZSK
2	AMSTA-TSL, Technical Library
	Commander, White Sands Missile Range, NM 88002
1	ATTN: STEWS-WS-VT
	President, Airborne, Electronics and Special Warfare Board, Fort Bragg, NC 28307
1	ATTN: Library
	Director, U.S. Army Ballistic Research Laboratory, Aberdeen Proving Ground, MD 21005
1	ATTN: SLCBR-TSB-S (STINFO)
	Commander, Dugway Proving Ground, Dugway, UT 84022
1	ATTN: Technical Library, Technical Information Division
	Commander, Harry Diamond Laboratories, 2800 Powder Mill Road, Adelphi, MD 20783
1	ATTN: Technical Information Office
	Director, Benet Weapons Laboratory, LCWSL, USA AMCCOM, Watervliet, NY 12189
1	ATTN: AMSMC-LCB-TL
1	AMSMC-LCB-R
1	AMSMC-LCB-RM
1	AMSMC-LCB-RP
	Commander, U.S. Army Foreign Science and Technology Center, 220 7th Street, N.E., Charlottesville, VA 22901-5396
3	ATTN: AIFRTC, Applied Technologies Branch, Gerald Schlesinger

No. of Copies	To
	Commander, U.S. Army Aeromedical Research Unit, P.O. Box 577, Fort Rucker, AL 36360
1	ATTN: Technical Library
	Commander, U.S. Army Aviation Systems Command, Aviation Research and Technology Activity, Aviation Applied Technology Directorate, Fort Eustis, VA 23604-5577
1	ATTN: SAVDL-E-MOS
	U.S. Army Aviation Training Library, Fort Rucker, AL 36360
1	ATTN: Building 5906-5907
	Commander, U.S. Army Agency for Aviation Safety, Fort Rucker, AL 36362
1	ATTN: Technical Library
	Commander, USACDC Air Defense Agency, Fort Bliss, TX 79916
1	ATTN: Technical Library
	Commander, U.S. Army Engineer School, Fort Belvoir, VA 22060
1	ATTN: Library
	Commander, U.S. Army Engineer Waterways Experiment Station, P. O. Box 631, Vicksburg, MS 39180
1	ATTN: Research Center Library
	Commandant, U.S. Army Quartermaster School, Fort Lee, VA 23801
1	ATTN: Quartermaster School Library
	Naval Research Laboratory, Washington, DC 20375
1	ATTN: Code 5830
2	Dr. G. R. Yoder - Code 6384
	Chief of Naval Research, Arlington, VA 22217
1	ATTN: Code 471
1	Edward J. Morrissey, WRDC/MLTE, Wright-Patterson Air Force, Base, OH 45433-6523
	Commander, U.S. Air Force Wright Research & Development Center, Wright-Patterson Air Force Base, OH 45433-6523
1	ATTN: WRDC/MLLP, M. Forney, Jr.
1	WRDC/MLBC, Mr. Stanley Schulman
	NASA - Marshall Space Flight Center, MSFC, AL 35812
1	ATTN: Mr. Paul Schuerer/EH01
	U.S. Department of Commerce, National Institute of Standards and Technology, Gaithersburg, MD 20899
1	ATTN: Stephen M. Hsu, Chief, Ceramics Division, Institute for Materials Science and Engineering
1	Committee on Marine Structures, Marine Board, National Research Council, 2101 Constitution Ave., N.W., Washington, DC 20418
1	Librarian, Materials Sciences Corporation, 930 Harvest Drive, Suite 300, Blue Bell, PA 19422
1	The Charles Stark Draper Laboratory, 68 Albany Street, Cambridge, MA 02139
	Wyman-Gordon Company, Worcester, MA 01601
1	ATTN: Technical Library
	Lockheed-Georgia Company, 86 South Cobb Drive, Marietta, GA 30063
1	ATTN: Materials and Processes Engineering Dept. 71-11, Zone 54
	General Dynamics, Convair Aerospace Division, P.O. Box 748, Fort Worth, TX 76101
1	ATTN: Mfg. Engineering Technical Library
	Director, U.S. Army Materials Technology Laboratory, Watertown, MA 02172-0001
2	ATTN: SLCMT-TML
2	Authors

U.S. Army Materials Technology Laboratory
Watertown, Massachusetts 02172-0001
Steven M. Serabian, and Donald J. Jaklitsch
A DETERMINATION/VALIDATION OF AUTOCLAVE FORCED CONVECTION HEATING

AD__________
UNCLASSIFIED
UNLIMITED DISTRIBUTION

Technical Report MTL TR 90-63, December 1990, 21 pp-illus-tables, D/A Project: IL162105AH84
AMCMS Code: 612105.AH840011

Key Words

Autoclave
Curing
Forced convection

The top face of a semi-infinite, plaster of paris slab was heated by forced convection in an autoclave while its depthwise temperature profile was obtained as a function of time by embedded thermocouples. The average forced convection heat transfer parameter of the slab's top face was determined from a time dependent lumped parameter analysis of temperature data acquired from two slug meters of varying design. The resulting nonlinear convective boundary conditions were applied to a transient heat transfer model of the semi-infinite slab to predict depthwise temperature profiles as a function of time. The model's thermal property data base was developed using a flash pulse method to determine thermal diffusivity and differential scanning calorimetry (DSC) to determine specific heat. Model temperatures compared poorly to experimental temperatures using the convective boundary condition obtained from the conventional wood slug meter design. However, a 5% temperature comparison was observed using the convective boundary condition obtained from the hybrid cork/fiberglass slug meter design. Finite element heat transfer analysis of the slug meters themselves illustrated the effects of heat retention on slug meter performance.

U.S. Army Materials Technology Laboratory
Watertown, Massachusetts 02172-0001
Steven M. Serabian, and Donald J. Jaklitsch
A DETERMINATION/VALIDATION OF AUTOCLAVE FORCED CONVECTION HEATING

AD__________
UNCLASSIFIED
UNLIMITED DISTRIBUTION

Technical Report MTL TR 90-63, December 1990, 21 pp-illus-tables, D/A Project: IL162105AH84
AMCMS Code: 612105.AH840011

Key Words

Autoclave
Curing
Forced convection

The top face of a semi-infinite, plaster of paris slab was heated by forced convection in an autoclave while its depthwise temperature profile was obtained as a function of time by embedded thermocouples. The average forced convection heat transfer parameter of the slab's top face was determined from a time dependent lumped parameter analysis of temperature data acquired from two slug meters of varying design. The resulting nonlinear convective boundary conditions were applied to a transient heat transfer model of the semi-infinite slab to predict depthwise temperature profiles as a function of time. The model's thermal property data base was developed using a flash pulse method to determine thermal diffusivity and differential scanning calorimetry (DSC) to determine specific heat. Model temperatures compared poorly to experimental temperatures using the convective boundary condition obtained from the conventional wood slug meter design. However, a 5% temperature comparison was observed using the convective boundary condition obtained from the hybrid cork/fiberglass slug meter design. Finite element heat transfer analysis of the slug meters themselves illustrated the effects of heat retention on slug meter performance.

U.S. Army Materials Technology Laboratory
Watertown, Massachusetts 02172-0001
Steven M. Serabian, and Donald J. Jaklitsch
A DETERMINATION/VALIDATION OF AUTOCLAVE FORCED CONVECTION HEATING

AD__________
UNCLASSIFIED
UNLIMITED DISTRIBUTION

Technical Report MTL TR 90-63, December 1990, 21 pp-illus-tables, D/A Project: IL162105AH84
AMCMS Code: 612105.AH840011

Key Words

Autoclave
Curing
Forced convection

The top face of a semi-infinite, plaster of paris slab was heated by forced convection in an autoclave while its depthwise temperature profile was obtained as a function of time by embedded thermocouples. The average forced convection heat transfer parameter of the slab's top face was determined from a time dependent lumped parameter analysis of temperature data acquired from two slug meters of varying design. The resulting nonlinear convective boundary conditions were applied to a transient heat transfer model of the semi-infinite slab to predict depthwise temperature profiles as a function of time. The model's thermal property data base was developed using a flash pulse method to determine thermal diffusivity and differential scanning calorimetry (DSC) to determine specific heat. Model temperatures compared poorly to experimental temperatures using the convective boundary condition obtained from the conventional wood slug meter design. However, a 5% temperature comparison was observed using the convective boundary condition obtained from the hybrid cork/fiberglass slug meter design. Finite element heat transfer analysis of the slug meters themselves illustrated the effects of heat retention on slug meter performance.

U.S. Army Materials Technology Laboratory
Watertown, Massachusetts 02172-0001
Steven M. Serabian, and Donald J. Jaklitsch
A DETERMINATION/VALIDATION OF AUTOCLAVE FORCED CONVECTION HEATING

AD__________
UNCLASSIFIED
UNLIMITED DISTRIBUTION

Technical Report MTL TR 90-63, December 1990, 21 pp-illus-tables, D/A Project: IL162105AH84
AMCMS Code: 612105.AH840011

Key Words

Autoclave
Curing
Forced convection

The top face of a semi-infinite, plaster of paris slab was heated by forced convection in an autoclave while its depthwise temperature profile was obtained as a function of time by embedded thermocouples. The average forced convection heat transfer parameter of the slab's top face was determined from a time dependent lumped parameter analysis of temperature data acquired from two slug meters of varying design. The resulting nonlinear convective boundary conditions were applied to a transient heat transfer model of the semi-infinite slab to predict depthwise temperature profiles as a function of time. The model's thermal property data base was developed using a flash pulse method to determine thermal diffusivity and differential scanning calorimetry (DSC) to determine specific heat. Model temperatures compared poorly to experimental temperatures using the convective boundary condition obtained from the conventional wood slug meter design. However, a 5% temperature comparison was observed using the convective boundary condition obtained from the hybrid cork/fiberglass slug meter design. Finite element heat transfer analysis of the slug meters themselves illustrated the effects of heat retention on slug meter performance.